Electronic Supplementary Material (ESI) for Journal of Materials Chemistry A.


# Tungsten-Based Porous Thin-Films for Electrocatalytic Hydrogen Generation—Electronic Supplementary Information

*Huilong Fei,[†,#] Yang Yang,[†,‡,#] Xiujun Fan,[‡] Gunuk Wang,[†] Gedeng Ruan[†] and James M. Tour[†,‡,¶,*]*

[†]*Department of Chemistry,* [‡]*Richard E. Smalley Institute for Nanoscale Science and Technology,* [¶]*Department of Materials Science and NanoEngineering, Rice University, 6100 Main Street, Houston, Texas 77005, USA*

[#]These authors contributed equally to this work.

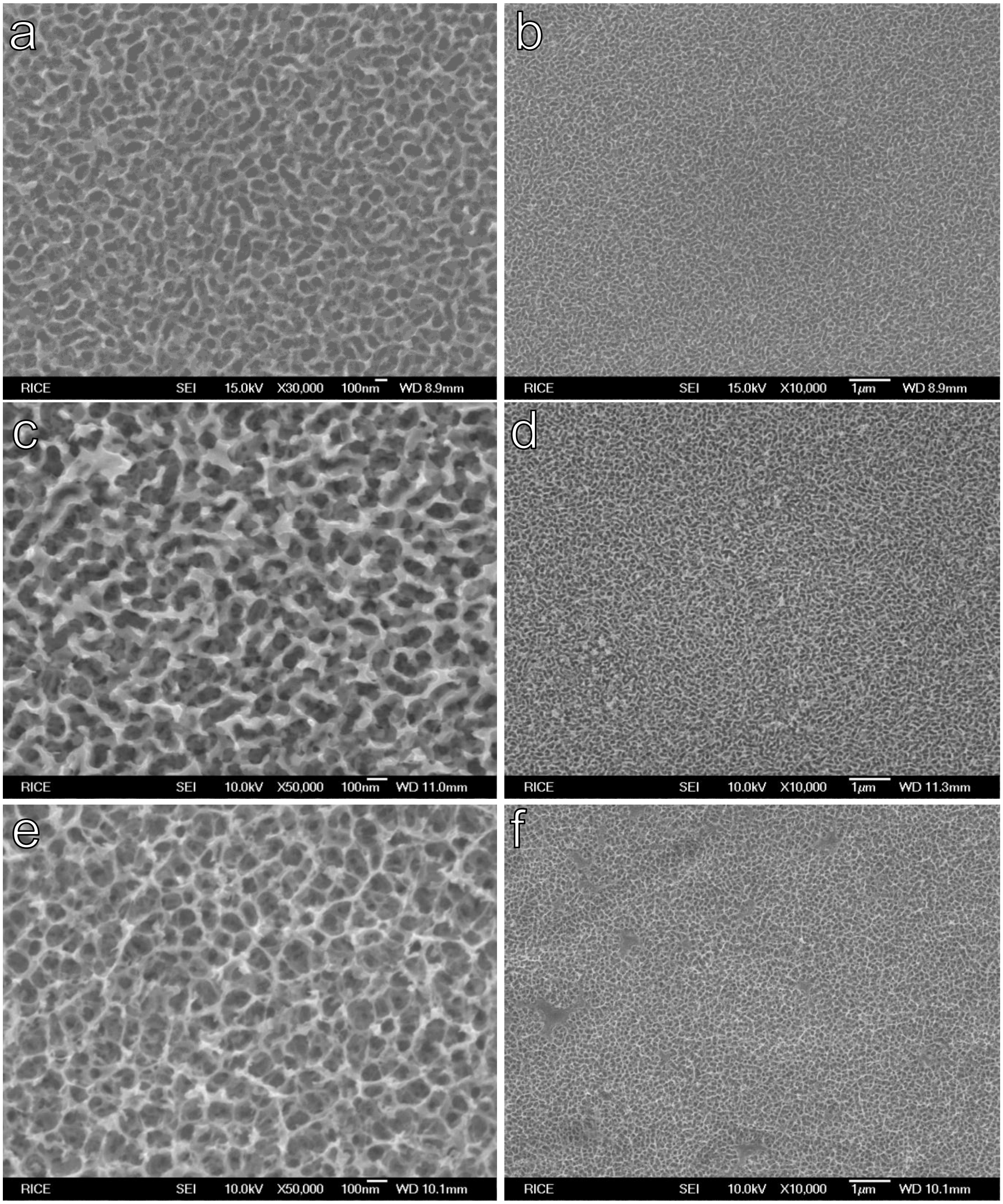

**Figure S1**. SEM images of (a-b) PWO, (c-d) PWS, (e-f) PWC at lower magnifications, suggesting the uniform porous structures of these films across the treated areas.

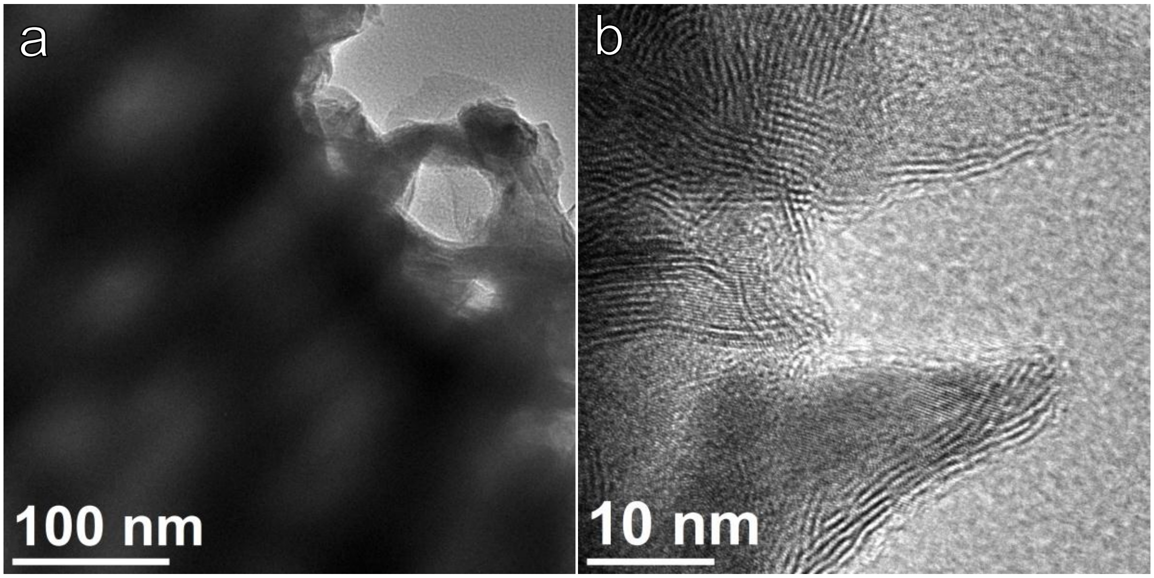


**Figure S2.** TEM images of PWS at (a) low and (b) high magnifications.

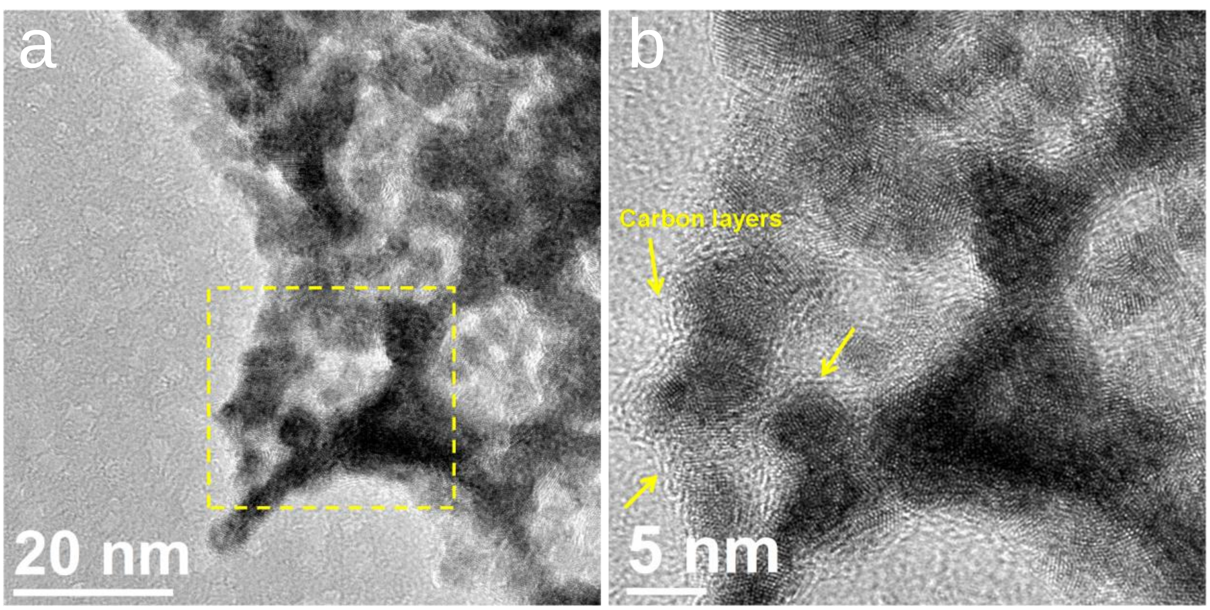


**Figure S3.** (a) TEM image of PWC, showing that the PWC are composed of interconnected nanoparticles. (b) Enlarged view of the squared area in (a), which shows the carbon layers surrounding the WC nanoparticles.

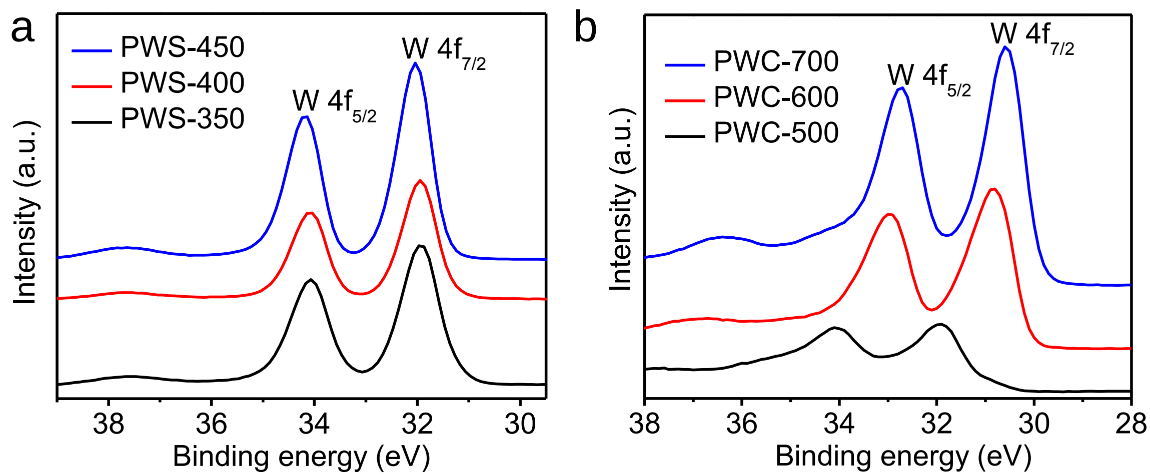


**Figure S4.** XPS spectra of W 4f for (a) PWS and (b) PWC synthesized at different temperatures. The PWC-500 shows broadened peaks and have higher binding energy compared to PWC-600 and PWC-700, suggesting that the conversion from oxide to carbide at 500 °C is incomplete.

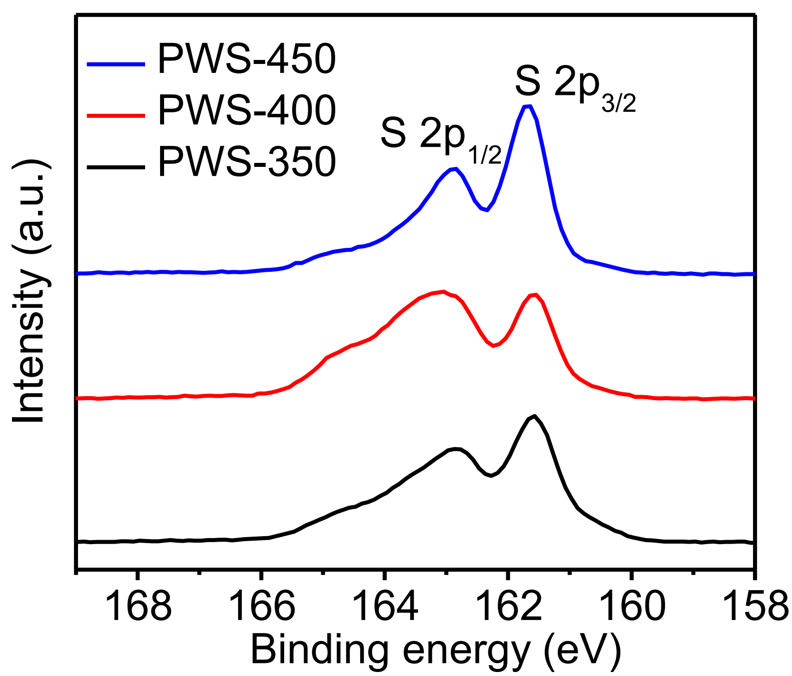


**Figure S5.** XPS spectra of S 2p for PWS-350, PWS-400 and PWS-450.

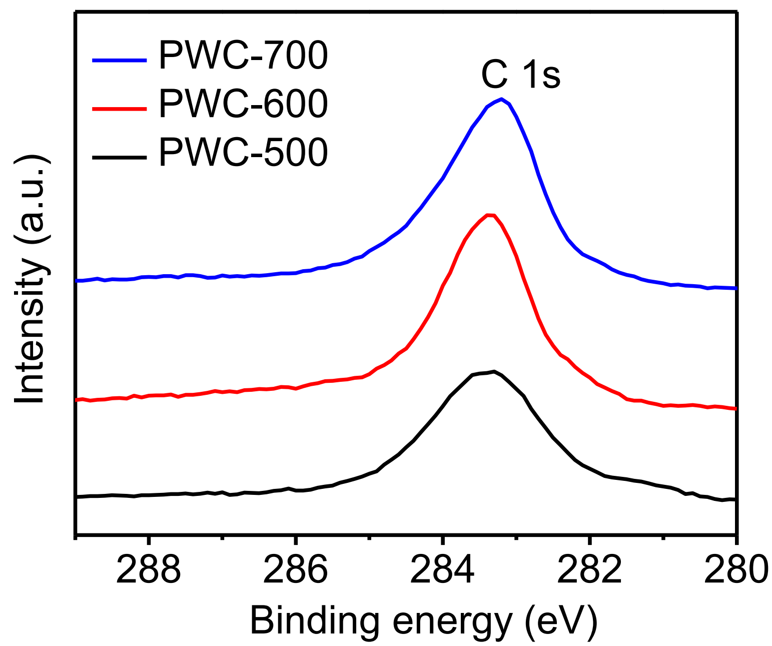


**Figure S6.** XPS spectra of C 1s for PWC-500, PWC-600 and PWC-700.

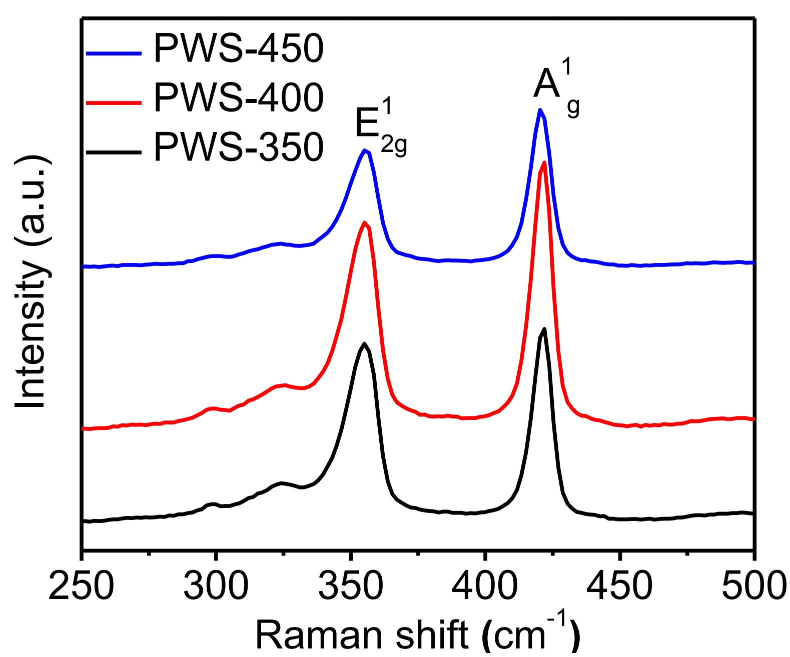


**Figure S7.** Raman spectra for PWS-350, PWS-400 and PWS-450, all of which show the characteristic $E^1_{2g}$ and $A^1_g$ vibration modes.

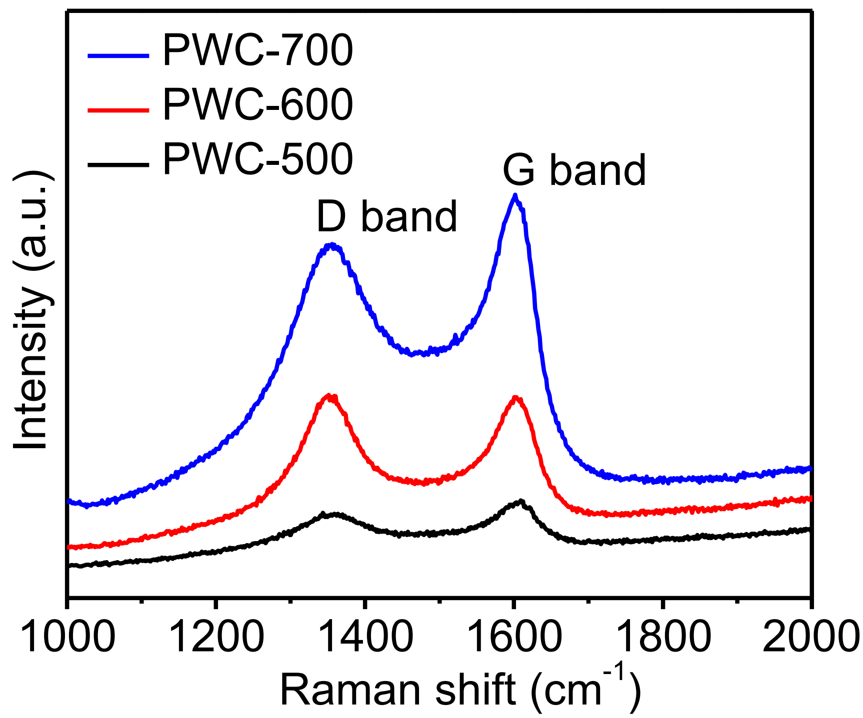


**Figure S8.** Raman spectra for PWC-500, PWC-600 and PWC-700, all of which show the characteristic D band and G band of carbon with larger peak intensity at higher synthesis temperature.

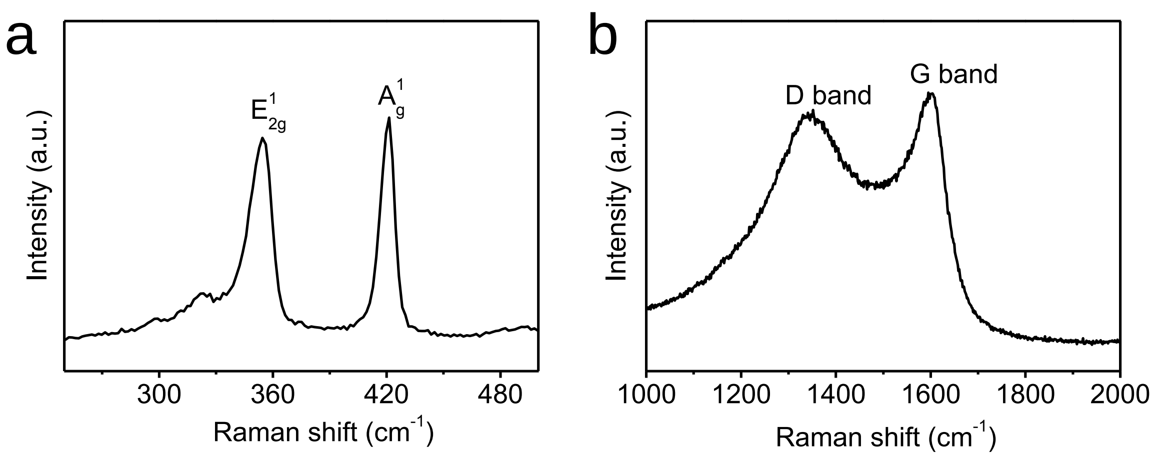


**Figure S9.** Raman spectra of the (a) NPWS and (b) NPWC

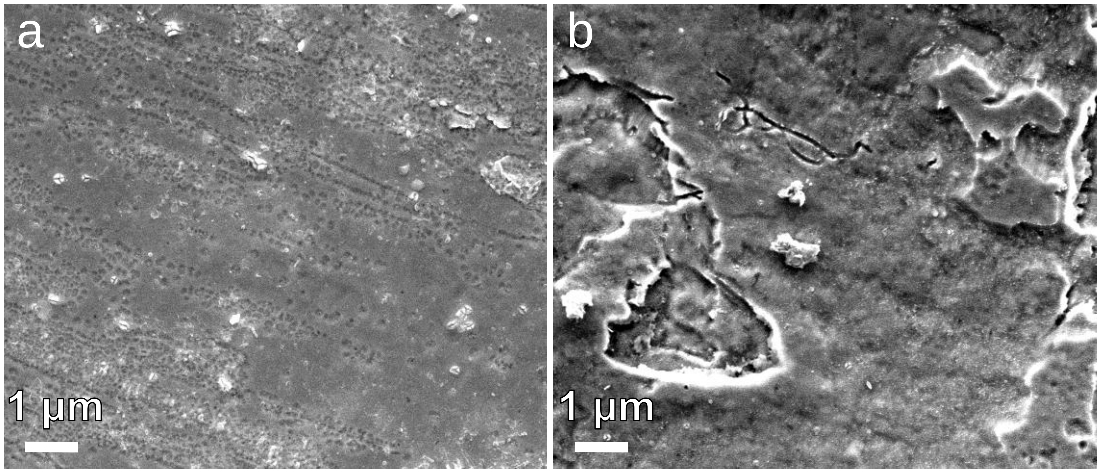


**Figure S10.** SEM images of the (a) NPWS and (b) NPWC.

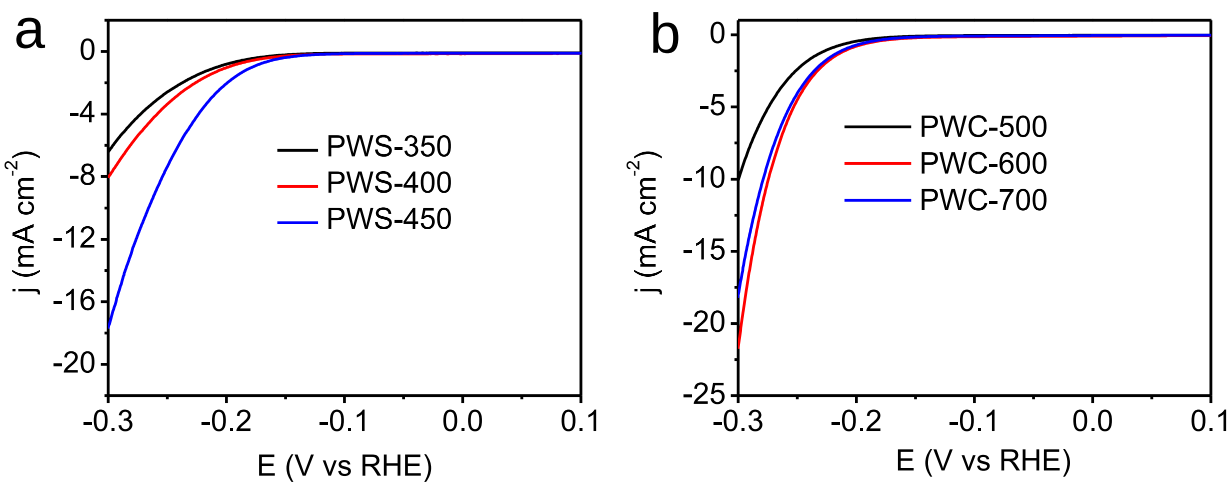


**Figure S11.** LSV polarization curves of (a) PWS and (b) PWC samples synthesized at different temperatures.

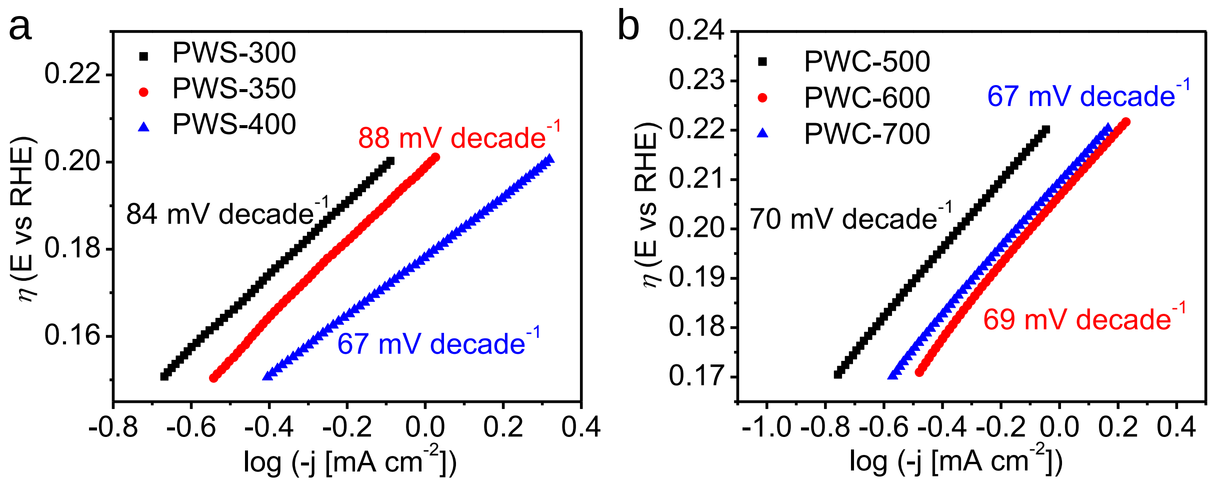


**Figure S12.** Tafel plots of (a) PWS and (b) PWC samples synthesized at different temperatures.

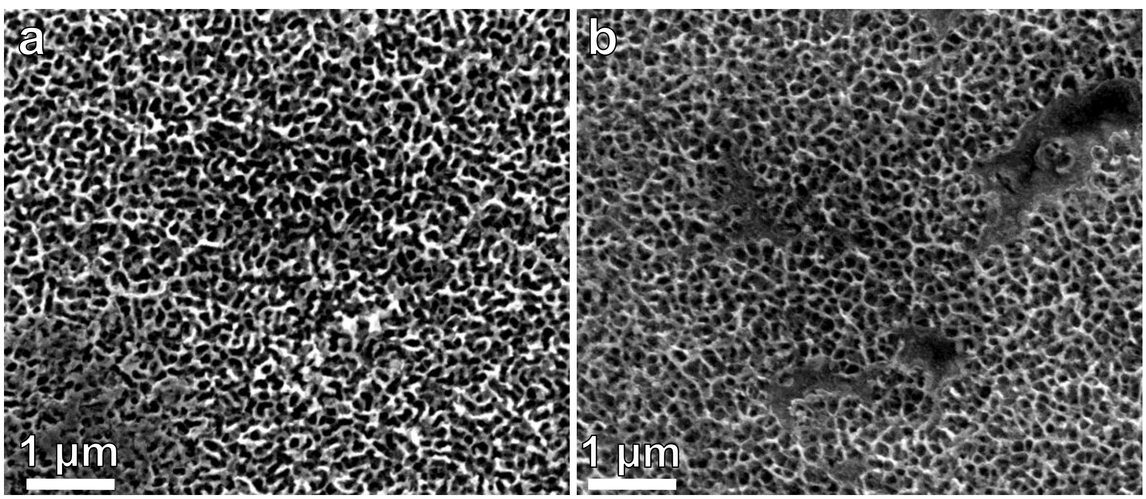

**Figure S13.** Morphologic characterization of the porous thin films after stability tests. SEM images of the (a) initial PWS and (b) PWC after stability tests.

**Table S1. Comparison of the HER activities of reported electrocatalysts.**

| Catalyst | Mass loading (μg $cm^{-2}$) | Onset overpotential (mV) | Tafel slope (mV | Overpotential for 10 mA $cm^{-2}$ (mV)[a] | Reference |
|---|---|---|---|---|---|

| | | | | | |
|---|---|---|---|---|---|
| | | | decade$^{-1}$) | | |
| Porous $WS_2$ thin film | ~ 80 | ~ 100 | 67 | 265 | This work |
| Porous WC thin film | ~ 160 | ~ 120 | 67 | 274 | This work |
| $WS_2$ nanosheets | 285 | ~ 60 | 72 | ~ 156 | 1 |
| $WS_2$/rGO sheets | 400 | 150 – 200 | 58 | ~ 275 | 2 |
| 1T-$WS_2$ nanosheets | NG | ~ 100 | 60 | ~ 250 | 3 |
| 1T-$WS_2$ nanosheets ($WS_2$ prepared by CVD method) | ~ 1000 | ~ 75 | 70 | ~ 142 | 4 |
| Ultrathin $WS_2$ nanoflakes | 350 | ~ 100 | 48 | ~ 180 | 5 |
| Nano-sized WC on carbon black | ~ 740 | ~ 165[b] | NG | ~ 255 | 6 |

[a] Most of the values are estimations on the basis of polarization curves. [b] The value is determined at current density of 1 mA cm$^{-2}$.

**References**


1. Wu, Z. Z.; Fang B. Z.; Bonakdarpour A.; Sun A. K.; Wilkinson D. P.; Wang D. Z. $WS_2$ Nanosheets as A Highly Efficient Electrocatalyst for Hydrogen Evolution Reaction. *Appl. Catal. B* **2012**, *125*, 59-66.
2. Yang, J.; Voiry, D.; Ahn, S. J.; Kang, D.; Kim, A. Y.; Chhowalla, M.; Shin, H. S. Two-Dimensional Hybrid Nanosheets of Tungsten Disulfide and Reduced

Graphene Oxide as Catalysts for Enhanced Hydrogen Evolution. Angew. *Chem. Int. Ed.* **2013**, *52*, 13751-13754.

3. Voiry, D.; Yamaguchi, H.; Li, J.; Silva, R.; Alves, D. C. B.; Fujita, T.; Chen, M.; Asefa, T.; Shenoy, V. B.; Eda, G.; Chhowalla, M. Enhanced Catalytic Activity in Strained Chemically Exfoliated $WS_2$ Nanosheets for Hydrogen Evolution. *Nat. Mater. 2013*, **12**, 850-855.
4. Lukowski, M. A.; Daniel, A. S.; English, C. R.; Meng, F.; Forticaux, A.; Hamers, R.; Jin, S. Highly Active Hydrogen Evolution Catalysis from Metallic $WS_2$ Nanosheets. *Energy Environ. Sci.* **2014**, *7*, 2608-2613.
5. Cheng, L.; Huang, W.; Gong, Q.; Liu, C.; Liu, Z.; Li, Y.; Dai, H. Ultrathin $WS_2$ Nanoflakes as a High-Performance Electrocatalyst for the Hydrogen Evolution Reaction. *Angew. Chem. Int. Ed.* **2014**, *53*, 7860-7863.
6. Ganesan, R.; Lee, J. S. Tungsten Carbide Microspheres as a Noble-Metal-Economic Electrocatalyst for Methanol Oxidation. *Angew. Chem. Int.. Ed.* **2005**, *44*, 6557-6560.